CHEMISTRY OF MATERIALS

ARTICLE

pubs.acs.org/cm

Investigation of Extra-Large Pore Zeolite Synthesis by a High-Throughput Approach

Jiuxing Jiang,[†] Yan Xu,[†] Peng Cheng,[†] Qiming Sun,[†] Jihong Yu,*[,†] Avelino Corma,[§] and Ruren Xu[†]

[†]State Key Lab of Inorganic Synthesis and Preparative Chemistry, College of Chemistry, Jilin University, Changchun 130012, P. R. China

[§]Instituto de Tecnología Química (UPV-CSIC), Universidad Politécnica de Valencia, Consejo Superior de Investigaciones Científicas, Av. de los Naranjos s/n, 46022 Valencia, Spain

Supporting Information

ABSTRACT: Seven isoindoline-based organic structure directing agents (OSDAs) with increasing sizes have been prepared and each applied in a high throughput (HT) design of $3^3 \times 5$ experiments by varying the synthesis parameters such as Si/Ge, Al(B)/(Si+Ge), F^-/(Si+Ge), and H_2O/(Si+Ge). Among the 945 experiments, 395 lead to crystalline zeolite products, corresponding to eight zeolites, i.e., Beta (3D 12 × 12 × 12 ring), ITQ-7 (3D 12 × 12 × 12 ring), ITQ-17 (3D 12 × 12 × 12 ring), ITQ-15 (2D 14 × 12 ring), ITQ-21 (3D 12 × 12 × 12 ring), ITQ-37(3D 30 ring), ITQ-43 (3D 28 × 12 × 12 ring), and ITQ-44 (3D 18 × 12 × 12 ring). Most of the crystalline phases obtained (85.8%, 339 of 395) are Beta, ITQ-7, ITQ-17, and intergrowths of ITQ-7 and ITQ-17, which have been named as "Default Structures" here. It has been found that concentrated gels and high Ge/Si ratio favor the formation of low framework density structures. When the OSDAs are relatively small, only "Default Structures" can be obtained, while if the size of OSDA increases above a certain dimension, extra-large pore zeolites such as ITQ-15, ITQ-37, ITQ-44, and ITQ-43 start to appear. The mesoporous chiral zeolite ITQ-37 has been successfully synthesized here with a much less costly achiral template than the one used originally. It has also been found that there is an intergrowth of ITQ-7 and ITQ-17 due to their closely correlated structures.

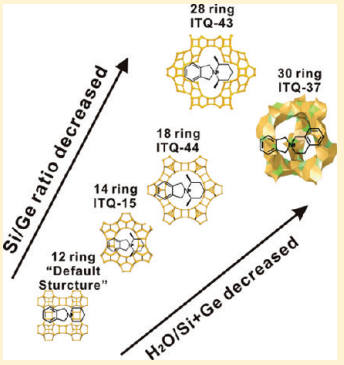

KEYWORDS: extra-large pore, high throughput, zeolite, synthesis, template

INTRODUCTION

Zeolites are crystalline porous materials formed by TO_4 tetrahedra (T = Si, P, Al, Ge, etc.) that present a large variety of industrial applications.[1−3] The discovery of zeolites with new structures and compositions to fulfill specific catalytic applications is a key issue in zeolite synthesis. Zeolites are normally prepared under hydrothermal conditions in which gel composition, structure directing agent (SDA), crystallization temperature, and time, etc., are critical parameters.[4] However, the relationship between the synthetic variables and the particular zeolite structures formed is not yet clearly understood because of the metastable nature of zeolites and the complexity of the formation mechanism.[5] The application of high-throughput (HT) approaches to materials science can help researchers to fast screen the variables involved in the synthetic process, increasing the number of samples produced and characterized.[6] Since 1998 Wendelbo and co-workers[7] introduced the HT technique into zeolite synthesis, this method has demonstrated its powerful strength in fast optimization of the synthetic conditions of known zeolites[8−10] as well as in the discovery of new structures.[11−13]

Extra-large pore zeolites are defined as those with pore aperture larger than 12 rings,[14] which in principle, can adsorb and react larger molecules. So far, among the 197 zeolite frameworks registered by the International Zeolite Association (each has been assigned with a three-letter code),[15] a relatively small number of zeolites, with 14 and 18 ring pores such as AlPO-8[16] (AET,14 ring), UTD-1[17] (DON, 14 ring), CIT-5[18] (CFI, 14 ring), SSZ-53[19] (SFH, 14 ring), SSZ-59[19] (SFN, 14 ring), OSB-1[20] (OSO, 14 ring), ITQ-15[21]/IM-12[22] (UTL, 14 × 12 ring), VPI-5[23] (VFI, 18 ring), and ECR-34[24] (ETR, 18 ring) have been obtained. Besides the above structures an important group of tridimensional extra-large pore zeolites such as cloverite (CLO, 3D 20 ring),[25] ITQ-33[12] (3D 18 × 10 × 10 ring), ITQ-40[26] (3D 16 × 16 × 15 ring), ITQ-44[13] (IRR 3D 18 × 12 × 12 ring), and the first mesoporous chiral zeolite ITQ-37[27] (ITV, 3D 30 ring) have also been obtained. Most recently, the first hierarchical meso-microporous zeolite ITQ-43[28] (3D 28 × 12 × 12 ring) has been reported. In the case of ITQ extra-large pore zeolites the structure directing role of Ge toward D4R and D3R building units has been shown to be very important for successful crystallization.[13,26,29,30]

Recently, we have reviewed the synthesis and catalytic applications of extra-large pore zeolites[31] and described three issues to successfully synthesize novel extra-large pore zeolites. They are as follows: i) large and rigid organic structure directing agents (OSDAs) with the required polarity favor the formation of

Received: April 28, 2011
Revised: September 15, 2011
Published: October 12, 2011

Table 1. OSDA1-7 Used in the Synthesis

OSDA	Nomenclature	Structure Formula	C/N
OSDA1	spiro[isoindoline-2,1'-piperidin]-1'-ium	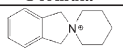	13
OSDA2	4'-methylspiro[isoindoline-2,1'-piperidin]-1'-ium	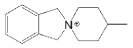	14
OSDA3	3'-methylspiro[isoindoline-2,1'-piperidin]-1'-ium	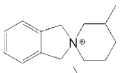	14
OSDA4	2'-methylspiro[isoindoline-2,1'-piperidin]-1'-ium	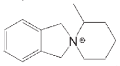	14
OSDA5	3',5'-dimethylspiro[isoindoline-2,1'-piperidin]-1'-ium	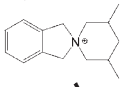	15
OSDA6	2',6'-methylspiro[isoindoline-2,1'-piperidin]-1'-ium	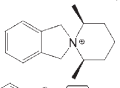	15
OSDA7	3',4'-dihydro-1'H-spiro [isoindoline-2,2'-isoquinolin]-2-ium	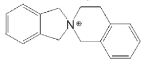	17

zeolites with larger micropore volume and a multidimensional channel system, though this is not a "sine qua non" requirement; ii) concentrated gels and fluoride media can increase the probabilities for producing structures with lower framework density (FD);[32] and iii) the synthesis of frameworks containing D4R and D3R can be facilitated by the introduction of some heteroatoms such as Ge. The presence of these secondary building units, together with the suitable OSDAs, will direct to the formation of structures with extra-large pores. In addition to those synthetic considerations, the application of high-throughput (HT) approaches to zeolite synthesis will also speed up the discovery of novel extra-large pore zeolites.

In the present work we have investigated the following issues: i) how small the difference in the structure of rigid OSDAs can alter the phase selectivity and ii) how the gel concentration, Si/Ge ratio, Al(B) incorporation, and F^- concentration affect the synthesis. To do that we have designed a series of OSDAs with increasing size based on isoindoline for the synthesis. Then for each OSDA, a $3^3 \times 5$ factorial design of experiments has been applied and HT synthesis approaches have been used for carrying out a systematic variation of the synthetic parameters. Following this methodology, further insight into the formation of extra-large pore zeolites has been provided.

EXPERIMENTAL SECTION

Syntheses of OSDAs. The OSDAs (see Table 1) have been prepared by a one step reaction in which 1,2-bis(bromomethyl)benzene and substituted piperidine were combined in a 1:1 molar ratio in the presence of an equal mole of K_2CO_3. The mixtures were heated under reflux for two days. The bromide was converted into the hydroxide form (OSDAOH) by ion exchange, and detailed information on the synthesis procedure can be seen in the Supporting Information.

Syntheses of Zeolites. An initial experimental factorial design ($3^3 \times 5$ for each OSDA) was performed in which Si/Ge, Al(B)/(Si+Ge), F^-/(Si+Ge), and H_2O/(Si+Ge) were selected as synthetic variables. Here we use Tecan CH Miniprep 75 laboratory robot system to dispense the liquid reagents. The typical synthesis procedure was as follows: First, the Telfon vials were put on the IKA RO 15 power 15 head magnetic stirrer in the robot box. Then the liquid reagents such as Ludox (SiO_2, 40%), OSDAOH, NH_4F (10 wt % in water solution), and NH_4Cl (10 wt % in water solution) were added by robot with stirring. After finishing adding

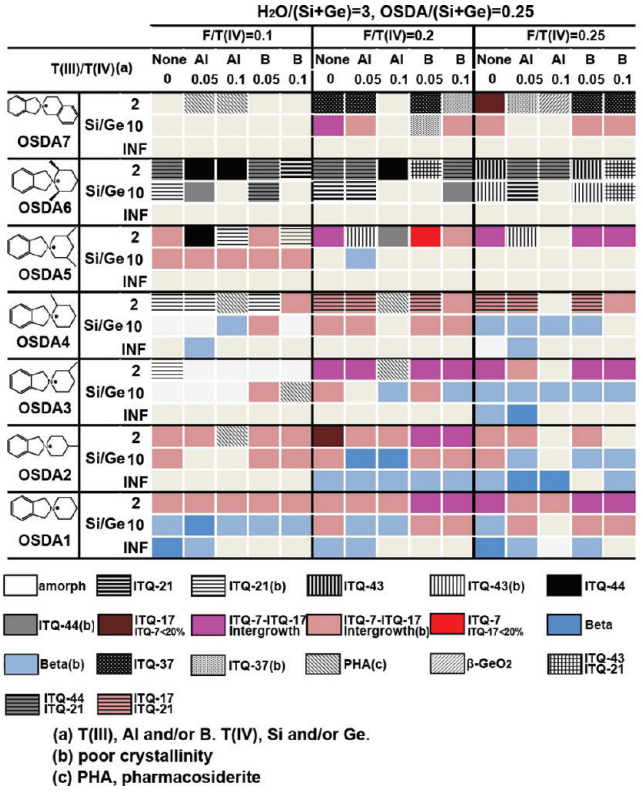

Figure 1. Crystallization field diagram for all 7 OSDAs at H_2O/(Si+Ge) = 3.

the liquid reagents, the solid sources, GeO_2 (99.998%) and/or Al_2O_3 (75 wt %, Catapal B), were added into the vials manually with stirring to form a homogeneous gel. All the vials were put under an infrared lamp to evaporate excess water until the desired water amount was achieved by weighing. Finally, 15 Teflon vials were inserted into a multiautoclave, and the crystallization was carried out at 175 °C for one week under static conditions.

Characterization Techniques. Scanning Electron Micrographs were obtained with a JEOL JSM-6700F Scanning Electronic Microscope. Samples were first analyzed with a Bruker D8 Discover X-ray diffractometer, and then those with special interest were further characterized with a Rigaku D/max 2500 X-ray diffractometer. ^1H (300 MHz) NMR spectra used for characterization of the prepared SDA were recorded on a Varian Mercury 300 spectrometer in D_2O solutions at ambient temperature.

RESULTS AND DISCUSSION

Crystallization Field Diagram. Each of the OSDAs was used in a $3^3 \times 5$ HT experimental design, in which the following synthetic variables were considered: Si/Ge (× 3, set to 2, 10, INF), Al(B)/(Si+Ge) (× 5, set to 0, 0.05, 0.1 for both Al and B), F^-/(Si+Ge) (× 3, set to 0.1, 0.2, 0.25), H_2O/(Si+Ge) (× 3, set to 3, 7, 15), and OSDA/(Si+Ge) was fixed to 0.25. A total of 945 synthesis experiments were performed. The resulting crystallization field diagrams are shown in Figures 1−3. 395 experiments gave rise to crystalline zeolite products, including eight zeolite phases, i.e., Beta (3D 12 × 12 × 12 ring), ITQ-7 (3D 12 × 12 × 12 ring), ITQ-17 (3D 12 × 12 × 12 ring), ITQ-15 (2D 14 × 12 ring), ITQ-21 (3D 12 × 12 × 12 ring), ITQ-37 (3D 30 ring), ITQ-43 (3D 28 × 12 × 12 ring), and ITQ-44 (3D 18 × 12 × 12 ring). Among the 395 crystalline zeolite products, 104 were found to be Beta, while 6 correspond to ITQ-7[30] (ITQ-17 < 20%),

dx.doi.org/10.1021/cm201221z |Chem. Mater. 2011, 23, 4709–4715

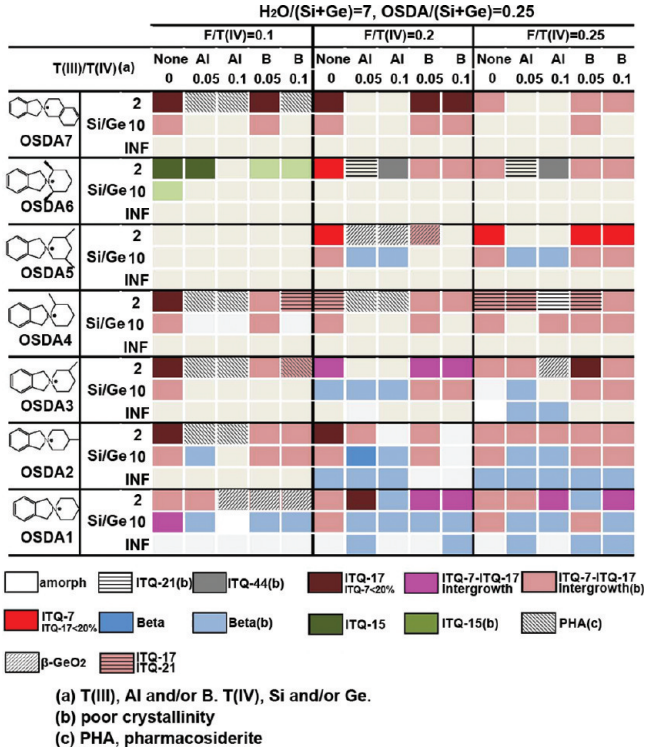

Figure 2. Crystallization field diagram for all 7 OSDAs at H_2O/(Si+Ge) = 7.

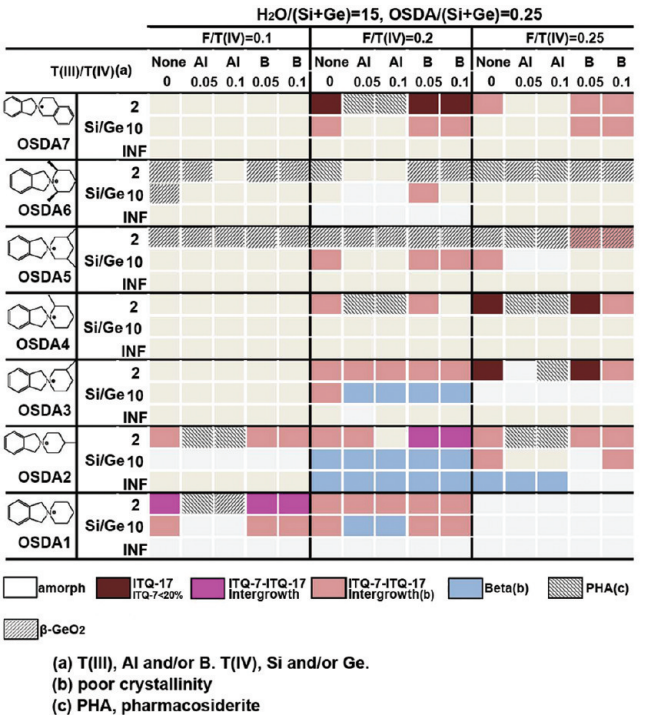

Figure 3. Crystallization field diagram for all 7 OSDAs at H_2O/(Si+Ge) = 15.

20 correspond to ITQ-17[33] (ITQ-7 < 20%), and 201 correspond to their intergrowths, 5 to ITQ-15,[21] 14 to ITQ-21,[34] 8 to ITQ-37,[27] 6 to ITQ-43, and 9 to ITQ-44.[13] Some experiments produced a mixture of two zeolite phases, including ITQ-44 and ITQ-21 (8 samples), ITQ-43 and ITQ-21 (3 samples), ITQ-21 and the ITQ-7/ITQ-17 intergrowth (11 samples). The XRD patterns and SEM images of the typical samples can be seen in Figure S1 and Figure S2, respectively.

Notably, among the 8 crystalline zeolite products that have been found, ITQ-15, ITQ-37, ITQ-44, and ITQ-43 possess extra-large pore channels. Particularly, the mesoporous chiral zeolite ITQ-37 with 30 ring channels has been now synthesized with a relatively simple achiral OSDA, while in the original synthesis[27] a more complex diquaternaryamonium with four chiral centers as OSDA was required.

Most of the crystalline phases (85.8%, 339 of 395) are Beta, ITQ-7, ITQ-17, and intergrowths of ITQ-7 and ITQ-17, so they have been named as "Default Structures".

Directing Effect of Ge toward Formation of Specific Secondary Building Units (SBUs). The presence of Ge in the synthesis can stabilize zeolite structures containing D4R SBU as demonstrated by means of theoretical calculations as well as experiments.[35,36] By using Electrospray Ionization Mass Spectrometry, Schüth and co-workers[37,38] demonstrate that the germanosilicate oligomer such as D4R and substituted D4R are formed immediately before nucleation. More recently, the incorporation of Ge in the synthesis has also shown its ability to induce the formation of structures with 3 ring (ITQ-33[12]), D3R (ITQ-44[13] and ITQ-40[26]), and spiro-5 (PKU-9[39] and GeGaO-CJ63[40]). A common explanation for this observation is based on the different coordination geometry of Si and Ge atom. In the case of pure siliceous structures, the average Si−O−Si bond angle is about 148°, which is not favorable for SUBs like D4R, 3 ring, D3R, and spiro-5. However, the smaller Ge−O−Ge or Si−O−Ge bond angles may release geometric stress and thus stabilize these SBUs. In our study, among the 8 zeolite phases obtained, there are 7 containing D4R, i.e., ITQ-7, ITQ-15, ITQ-17, ITQ-21, ITQ-37, ITQ-44, and ITQ-43, while ITQ-44 contains both D4R and the first observed D3R. The results confirm the strong structure-directing effect of Ge toward D4R and D3R. Besides, we can see (Figure 4a) that the number of zeolites obtained decreases when increasing the Si/Ge ratio, while the product distribution versus framework density (Figure 4b) shows that high Ge content, i.e., low Si/Ge ratio facilitates the formation of low framework density extra-large pore zeolites (ITQ-37, ITQ-44, and ITQ-43).

The Effect of Gel Concentration. Several works[32,41,42] showed that during the synthesis of high-silica zeolites low H_2O/SiO_2 ratio favored crystallization of zeolites with lower framework density (FD) in which high silica zeolite Beta (15.3 T atoms/1000 Å^3) and Chabazite (15.1 T atoms/1000 Å^3) were the lowest boundary.[32] Here we have focused on the syntheses of a number of germanosilicates, in which Beta zeolite is the highest FD boundary. For doing that, the influence of gel concentration of H_2O/(Si+Ge) = 3 (Figure 1), H_2O/(Si+Ge) = 7 (Figure 2), and H_2O/(Si+Ge) = 15 (Figure 3) for all seven OSDAs on the FD value of the resultant zeolite products has been compared. In these synthetic systems, 8 zeolite phases were identified, including Beta (15.3 T/1000 Å^3), ITQ-7 (15.4 T/1000 Å^3), ITQ-15 (14.5 T/1000 Å^3), ITQ-17 (14.6 T/1000 Å^3), ITQ-21 (11.6 T/1000 Å^3), ITQ-37 (10.3 T/1000 Å^3), ITQ-43 (11.4 T/1000 Å^3), and ITQ-44 (10.9 T/1000 Å^3). Figure 5a illustrates the distribution of crystalline products obtained with OSDA1-OSDA7. It shows that the number of crystalline product decreases when increasing the water content. The FD distribution in each group (Figure 5b) shows that, most of the low FD products, such as ITQ-37, ITQ-44, ITQ-43, and ITQ-21, are exclusively formed at H_2O/(Si+Ge) =

dx.doi.org/10.1021/cm201221z |Chem. Mater. 2011, 23, 4709–4715

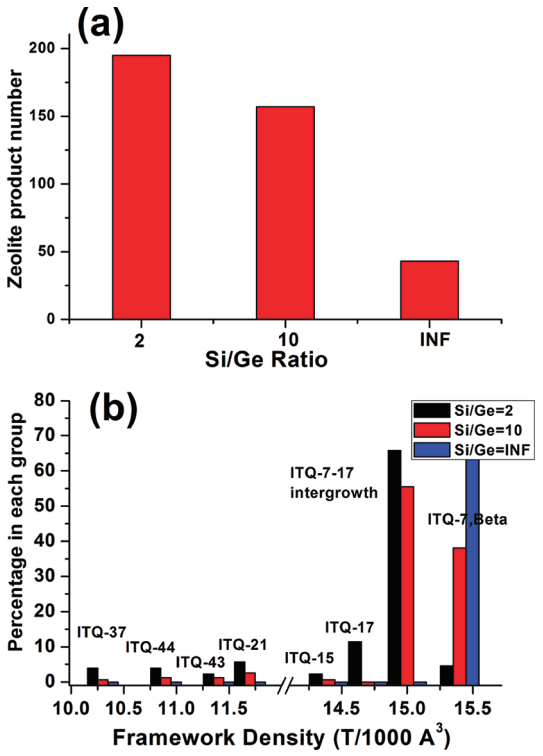

Figure 4. (a) The number of crystalline products for OSDA1−OSDA7 for three Si/Ge ratio groups (Si/Ge = 2, 10, INF). (b) The product distribution in percentage versus framework density within each group.

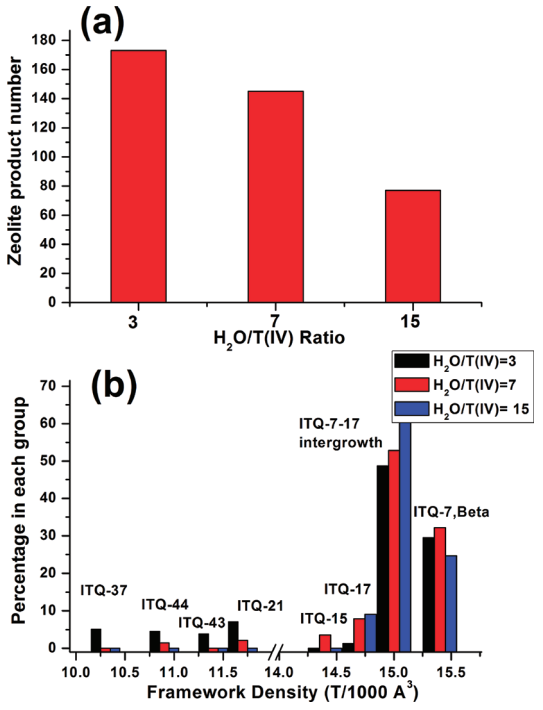

Figure 5. (a) The number of crystalline products for OSDA1−OSDA7 for three synthetic concentration groups ($H_2O/T(IV)$ = 3, 7, 15). (b) The product distribution in percentage versus framework density in percentage within each group.

3, while only a very small number of the experiments at $H_2O/(Si+Ge)$ = 7 give lower FD structures, and none is obtained at

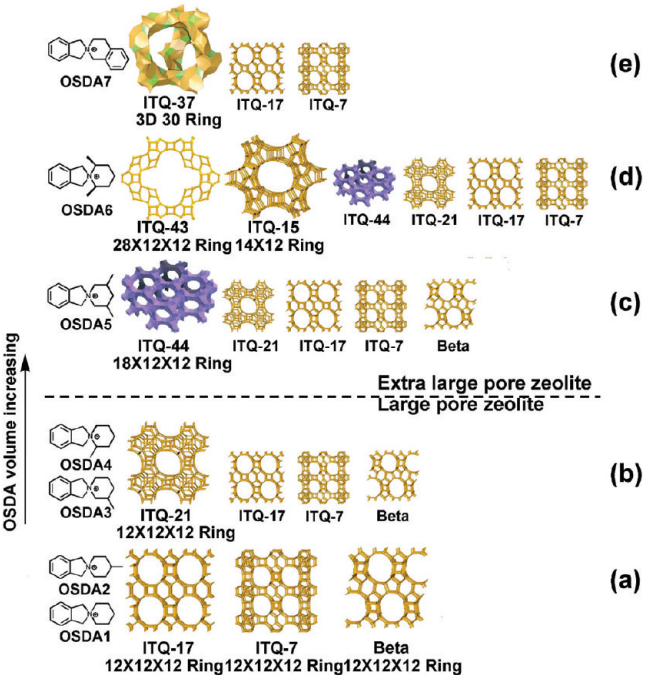

Figure 6. Converting "Default Structures" to extra-large pore zeolites. (a) OSDA1,2 can direct only the "Default Structures"; (b) Besides the "Default Structures", OSDA3,4 can produce ITQ-21; (c) When OSDA is increased to OSDA5, extra-large pore zeolite ITQ-44 starts to appear; (d) When OSDA6 is used, in addition to the structure mentioned above, it can induce the formation of ITQ-15 and ITQ-43; (e) When the largest OSDA7 is used, mesoporous chiral zeolite ITQ-37 is formed.

$H_2O/(Si+Ge)$= 15. ITQ-15 with an intermediate FD can only be obtained at the intermediate gel concentration, i.e., $H_2O/(Si+Ge)$ = 7, while high FD "Default Structures", i.e., ITQ-7, ITQ-17, their intergrowths, and Beta, are the most frequently observed phases in the three gel composition groups, being proportionally more abundant when working at $H_2O/(Si+Ge)$ = 7 and 15. From the above results, we can conclude that for germanosilicate zeolite synthesis, as it occurs with high silica zeolites concentrated gels favor the formation of low FD products.

OSDA Size Effect: Converting "Default Structures" to Extra-Large Pores. Davis and co-workers[43] studied the effect of the carbon to nitrogen ratio (C/N^+) in the OSDAs on the crystallization of zeolites. The authors concluded that relatively rigid OSDAs with moderate polarity, e.g., with C/N^+ between 11 and 16, appear to be the best option for high-silica zeolite synthesis. In some other works by Zones et al.,[42,44,45] it was found that when the OSDA increased up to a certain dimension (C/N^+ is about 10 for monoquaternary ammonium), the resultant products changed from clathrasils to microporous molecular sieves. This was in agreement with the study by Gies and coworkers[46,47] on the conditions of a successful OSDA to form clathrasil structures. Interestingly, in the present work, we observed the conversion from the high FD "Default Structures" to the extra-large pore zeolites when the size of OSDAs increases above a certain dimension (C/N^+ 15 and 17).

In germanosilicates, when an OSDA is relatively small or it is large but very flexible, the formation of "Default Structures" such as Beta, ITQ-7, and ITQ-17, are usually obtained. However when rigid OSDAs with increasing size have been studied it can be seen in Figure 6 that the smaller OSDA1 (C/N^+ = 13) and OSDA2

($C/N^+ = 14$) only direct to Beta, ITQ-7, and ITQ-17. In contrast, OSDA3, OSDA4 having the same C/N^+ as OSDA2 but with a larger size, directs toward ITQ-21 (FD = 11.6) which is a more open structure than ITQ-17 (FD = 14.6), although the synthesis product still contains some ITQ-17 impurity. When the size of the OSDA is further increased with a $C/N^+ = 15$, ITQ-44 (FD = 10.9) with 18 × 12 × 12 ring extra-large pores is obtained. If the OSDA6 ($C/N^+ = 15$) is adopted, besides ITQ-44, ITQ-15 with 14 × 12 ring extra-large pores and a novel meso-microporous zeolite ITQ-43 with 28 × 12 × 12 ring extra-large pores can also be found in the products. Notice that, Čejka and co-workers[48] have also reported the successful synthesis of ITQ-15 (UTL) using the analogues of OSDA5 and OSDA6. OSDA7 ($C/N^+ = 17$) is the largest OSDA used here, correspondingly, it directs the formation of the mesoporous zeolite ITQ-37.

The Effect of T^{III} Heteroatoms and the Concentration of Fluoride. The introduction of T^{III} (Al, B) has at least two effects on the synthesis. On the one hand, since T^{III}—O bond lengths and O—T^{III}—O bond angles are different from Si—O and O—Si—O, it may direct to some specific building units, thus inducing the formation of new structures. On the other hand, the negative charges generated by introduction of T^{III} elements in framework positions together with the F^- anion will require larger amounts of OSDA cations to be included in the pores, thus resulting in the increase of the micropore volume in the synthesized zeolite. According to the amount of aluminum that the product can accept, one can divide the zeolites into three groups: The first group corresponds to products that can only be crystallized in presence of Al, for instance, ITQ-44. The second group corresponds to zeolites that can only be obtained in a gel without Al or with small amount of Al, for example ITQ-37 and ITQ-43. The third group of zeolites is not strictly restricted by the Al content in the synthesis, for example, ITQ-7, ITQ-17, ITQ-15, and ITQ-21. Notably, ITQ-44 which belongs to the first group can only be synthesized at low F^- concentration. This might be due to the fact that when lower F^- anion content is introduced, more Al can be incorporated into the framework to compensate the positive charge of the OSDA required to fill pores, as requested for the formation of ITQ-44. On the other hand, ITQ-37 and ITQ-43 which belong to the second group can hardly be synthesized at a high Al concentration, and thus higher F^- concentration is required for compensating the large amount of OSDA incorporated.

The Intergrowth of ITQ-7 and ITQ-17. The structural relationship between ITQ-7 and ITQ-17 (the polymorph C of the Beta family) can be described as different stacking sequence of the same layer connected by the D4Rs (Figure 7). This close structural relationship raises the possibility of stacking faults and, particularly, a disordered intergrowth between ITQ-7 and ITQ-17 because of their similar tetragonal arrangement of D4R, which allows a perfect matching of the respective layers. The different degrees of intergrowth of the family ITQ-7 and ITQ-17 were simulated by Camblor and co-workers,[49] but there was no experimental evidence showing such intergrowth. Here we have first observed the intergrowth of ITQ-7 and ITQ-17 and a transformation from ITQ-7 to ITQ-17 when varying the synthetic conditions. Figure 8a shows the XRD powder pattern simulations of disordered intergrowths of the ITQ-7 and ITQ-17 family calculated using DIFFaX[50] developed by Treacy and Deem. The pure silica structure was used as input model for the simulations. The experimental XRD patterns showing the disordered intergrowths of the ITQ-7 and ITQ-17 family are given in Figure 8b. These samples are synthesized under different conditions by varying the type of OSDA, the $H_2O/(Si+Ge)$, Si/Ge, and $F^-/(Si+Ge)$.

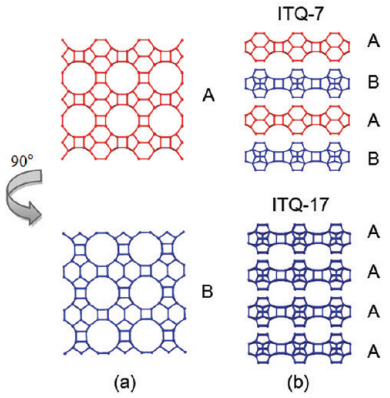

Figure 7. The structure relationship between ITQ-7 and ITQ-17. a) Layers A and B are related by 90° rotation. b) Layers of ITQ-7 and ITQ-17 are stacked in sequence of ABAB and AAAA, respectively.

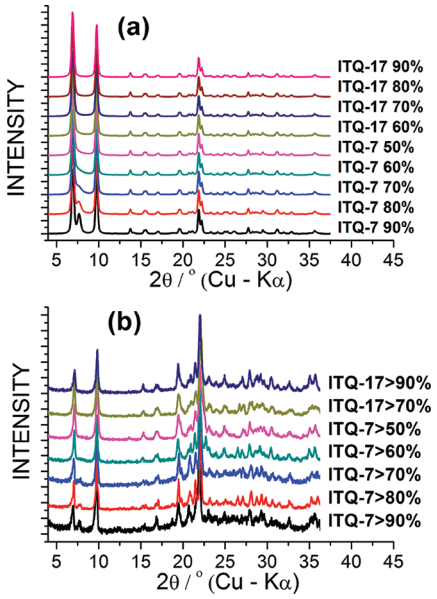

Figure 8. (a) XRD powder pattern simulations of disordered intergrowths of ITQ-7 and ITQ-17 family calculated by DIFFaX. (b) The experimental XRD powder patterns showing disordered intergrowths of ITQ-7 and ITQ-17 family. The synthetic conditions of samples from up to bottom: 1) $H_2O/(Si+Ge) = 7$, OSDA7, $Si/Ge = 2$, $F^-/(Si+Ge) = 0.2$; 2) $H_2O/(Si+Ge) = 7$, OSDA1, $Si/Ge = 2$, $F^-/(Si+Ge) = 0.2$, $Al/(Si+Ge) = 0.05$; 3) $H_2O/(Si+Ge) = 7$, OSDA3, $Si/Ge = 2$, $F^-/(Si+Ge) = 0.2$, $B/(Si+Ge) = 0.1$; 4) $H_2O/(Si+Ge) = 3$, OSDA3, $Si/Ge = 2$, $F^-/(Si+Ge) = 0.2$; 5) $H_2O/(Si+Ge) = 3$, OSDA2, $Si/Ge = 2$, $F^-/(Si+Ge) = 0.2$, $B/(Si+Ge) = 0.05$; 6) $H_2O/(Si+Ge) = 7$, OSDA5, $Si/Ge = 2$, $F^-/(Si+Ge) = 0.2$. 7) $H_2O/(Si+Ge) = 7$, OSDA5, $Si/Ge = 2$, $F^-/(Si+Ge) = 0.25$.

Unfortunately, we could not correlate this transformation with specific synthetic factors.

CONCLUSIONS

In the present work, seven OSDAs with increasing size based on the isoindoline have been prepared. Then a $3^3 \times 5$ HT factorial design for each OSDA has been performed, in which the following synthesis parameters including Si/Ge, Al(B)/(Si+Ge), $F^-/(Si+Ge)$, and $H_2O/(Si+Ge)$ have been considered. From a total of 945 synthesis experiments, 8 crystalline zeolite products

dx.doi.org/10.1021/cm201221z |Chem. Mater. 2011, 23, 4709–4715

have been obtained, including four large pore zeolites, i.e., Beta, ITQ-7, ITQ-17, and ITQ-21, four extra-large pore zeolites, i.e., ITQ-15, ITQ-37, ITQ-44, and ITQ-43. The results show that

a) The introduction of Ge can induce the formation of D4R and D3R SBUs which are beneficial factors to produce extra-large pore zeolites. Furthermore, a gel with lower Si/Ge ratio has more opportunities to crystallize as extra-large pore zeolites.
b) In germanosilicates, a lower $H_2O/(Si+Ge)$ ratio favors the synthesis of lower framework density zeolites, as it also occurs with Ge free high silica zeolites.
c) The smaller OSDAs can only produce "Default Structures", while larger and rigid OSDAs can direct toward extra-large pore zeolites.
d) Because both the incorporation of Al cations and the F^- anions present in the zeolite generate the negative charges, there appears a competition between the Al content and F^- in the synthesis. Less amount of F^- content may enable more Al cations to be incorporated into the framework, and vice versa.
e) Experimentally, there are disordered intergrowths in the family of ITQ-7 and ITQ-17 due to their close structural relationship.

■ ASSOCIATED CONTENT

Supporting Information. Detailed OSDA synthesis procedure, SEM images, and XRD patterns. This material is available free of charge via the Internet at http://pubs.acs.org.

■ AUTHOR INFORMATION

Corresponding Author
*E-mail: jihong@jlu.edu.cn.

■ ACKNOWLEDGMENT

This work is supported by the State Basic Research Project of China (Grants: 2011CB808703 and 2007CB936402), the National Natural Science Foundation of China, and the Major International Joint Research Project of China. A.C. thanks the project consolider Ingenio MULTICAT for financial support.

■ REFERENCES

(1) Venuto, P. B. *Microporous Mater.* **1994**, *2*, 297.
(2) Corma, A. *J. Catal.* **2003**, *216* (1−2), 298–312.
(3) Corma, A. *Chem. Rev.* **1995**, *95* (3), 559–614.
(4) Yu, J. Synthesis of zeolites. *Introduction to Zeolite Science and Practice*, 3rd revised ed.; Cejka, J., van Bekkum., H., Corma, A., Schüth., F., Eds.; *Studies in Surface Science and Catalysis* 168; Elsevier: Amsterdam, 2007; pp 39−103.
(5) Yu, J. H.; Xu, R. R. *Acc. Chem. Res.* **2003**, *36*, 481.
(6) Xiang, X. D.; Takeuchi., I. *Combinatorial Materials Science*; Eds.; Dekker: New York, 2003.
(7) Akporiaye, D. E.; Dahl, I. M.; Karlsson., A.; Wendelbo., R. *Angew. Chem., Int. Ed.* **1998**, *37*, 609–611.
(8) Corma, A.; Moliner, M.; Serra, J. M.; Serna, P.; Díaz-Cabañas., M. J.; Baumes, L. A. *Chem. Mater.* **2006**, *18*, 3287–3296.
(9) Klein, J.; Lehmann, C. W.; Schmidt, H. W.; Maier, W. F. *Angew. Chem., Int. Ed.* **1998**, *37*, 3369–3372.
(10) Choi, K.; Gardner, D.; Hilbrandt, N.; Bein, T. *Angew. Chem., Int. Ed.* **1999**, *38*, 2891–2894.
(11) Song, Y.; Yu., J.; Li, G.; Li, Y.; Wang, Y.; Xu, R. *Chem. Commun.* **2002**, 1720–1721.
(12) Corma, A.; Díaz-Cabañas., M. J.; Jorda, J. L.; Martinez, C.; Moliner, M. *Nature* **2006**, *443*, 842–845.
(13) Jiang, J. X.; Jorda, J. L.; Díaz-Cabañas, M. J.; Yu, J. H.; Corma, A. *Angew. Chem., Int. Ed.* **2010**, *49*, 4986–4988.
(14) Davis, M. E. *Chem.--Eur. J.* **1997**, *3*, 1745–1750.
(15) Baerlocher, Ch.; McCusker, L. B. Database of Zeolite Structures: http://www.iza-structure.org/databases/ (accessed August 27, 2011).
(16) Dessau, R. M.; Schlenker, J. L.; Higgins, J. B. *Zeolites* **1990**, *10*, 522–524.
(17) (a) Freyhardt, C. C.; Tsapatsis, M.; Lobo, R. F.; Balkus, K. J., Jr.; Davis, M. E. *Nature* **1996**, *381*, 295. (b) Lobo, R. F.; Tsapatsis, M.; Freyhardt, C. C.; Khodabandeh, S.; Wagner, P.; Chen, C. Y.; Balkus, K. J.; Zones, S. I.; Davis, M. E. *J. Am. Chem. Soc.* **1997**, *119* (36), 8474–8484. (c) Wessels, T.; Baerlocher, C.; McCusker, L. B.; Creyghton, E. J. *J. Am. Chem. Soc.* **1999**, *121*, 6242–6247.
(18) Wagner, P.; Yoshikawa, M.; Lovallo, M.; Tsuji, K.; Taspatsis, M.; Davis., M. E. *Chem Commun.* **1997**, 2179–2180.
(19) Burton, A.; Elomari, S.; Chen, C. Y.; Medrud, R. C.; Chan, I. Y.; Bull, L. M.; Kibby, C.; Harris, T. V.; Zones, S. I.; Vittoratos, E. S. *Chem.--Eur. J.* **2003**, *9*, 5737–5748.
(20) Cheetham, A. K.; Fjellvåg, H.; Gier, T. E.; Kongshaug, K. O.; Lillerud, K. P.; Stucky, G. D. *Stud. Surf. Sci. Catal.* **2001**, *135*, 158.
(21) Corma, A.; Díaz-Cabañas, M. J.; Rey, F.; Nicolopoulus, S.; Boulahya, K. *Chem. Commun.* **2004**, 1356–1357.
(22) Paillaud, J. L.; Harbuzaru, B.; Patarin, J.; Bats, N. *Science* **2004**, *304*, 990–992.
(23) Davis, M. E.; Saldarriaga, C.; Montes, C.; Garces, J. M.; Crowder, C. *Nature* **1988**, *331*, 698.
(24) Strohmaier, K. G.; Vaughan, D. E. W. *J. Am. Chem. Soc.* **2003**, *125*, 16035–16039.
(25) Estermann, M.; McCusker, L. B.; Baerlocher, C.; Merrouche, A.; Kessler, H. *Nature* **1991**, *352*, 320–323.
(26) Corma, A.; Díaz-Cabañas, M. J.; Jiang, J.; Afeworki, M.; Dorset, D. L.; Soled, S. L.; Strohmaier, K. G. *Proc. Natl. Acad. Sci. U.S.A.* **2010**, *107* (32), 13977–14002.
(27) Sun, J. L.; Bonneau, C.; Cantin, A.; Corma, A.; Díaz-Cabañas, M. J.; Moliner, M.; Zhang, D. L.; Li, M. R.; Zou, X. D. *Nature* **2009**, *458*, 1154–1159.
(28) Jiang, J.; Jorda, J. L.; Yu, J.; Baumes, L. A.; Mugnaioli, E.; Díaz-Cabañas, M. J.; Kolb, U.; Corma, A. *Science* **2011**, *333*, 1131.
(29) Corma, A.; Díaz-Cabañas, M. J.; Fornés, V. *Angew. Chem., Int. Ed.* **2000**, *39*, 2346.
(30) Villaescusa, L. A.; Barrett, P. A.; Camblor, M. A. *Angew. Chem., Int. Ed.* **1999**, *38*, 1997.
(31) Jiang, J.; Yu, J. H.; Corma, A. *Angew. Chem., Int. Ed.* **2010**, *49*, 3120–3145.
(32) Camblor, M. A.; Villaescusa, L. A.; Díaz-Cabañas, M. J. *Top. Catal.* **1999**, *9*, 59.
(33) Corma, A.; Navarro, M. T.; Rey, F.; Rius, J.; Valencia, S. *Angew. Chem., Int. Ed.* **2001**, *40*, 2277.
(34) (a) Corma, A.; Díaz-Cabañas, M. J.; Martínez-Triguero, J.; Rey, F.; Rius, J. *Nature* **2002**, *418*, 514.
(35) Blasco, T.; Corma, A.; Díaz-Cabañas, M. J.; Rey, F.; Rius, J.; Sastre, G.; Vidal-Moya, J. A. *J. Am. Chem. Soc.* **2004**, *126*, 13414–13423.
(36) Blasco, T.; Corma, A.; Díaz-Cabañas, M. J.; Rey, F.; Vidal-Moya., J. A.; Zicovich-Wilson., C. M. *J. Phys. Chem. B* **2002**, *106* (10), 2634–2642.
(37) Schaack, B. B.; Schrader, W.; Schüth, F. *Angew. Chem., Int. Ed.* **2008**, *47*, 9092–9095.
(38) Schaack, B. B.; Schrader, W.; Corma, A.; Schüth, F. *Chem. Mater.* **2009**, *21*, 4448–4453.
(39) Su, J.; Wang, Y. X.; Wang, Z. M.; Lin, J. H. *J. Am. Chem. Soc.* **2009**, *131*, 6080–6081.
(40) Han, Y. D.; Li, Y.; Yu, J. H.; Xu, R. R. *Angew. Chem, Int. Ed.* **2011**, *50*, 3003–3005.

(41) Camblor, M. A.; Barrett, P. A.; Díaz-Cabañas, M. J.; Villaescusa, L. A.; Puche, M.; Boix, T.; Perez, E.; Koller, H. *Microporous Mesoporous Mater.* **2001**, *48*, 11–22.
(42) Zones, S. I.; Burton, A. W.; Lee, G. S.; Olmstead, M. M. *J. Am. Chem. Soc.* **2007**, *129*, 9066–9079.
(43) Lobo, R. F.; Zones, S. I.; Davis, M. E. *J. Inclusion Phenom. Mol. Recognit. Chem.* **1995**, *21*, 47–78.
(44) Nakagawa, Y.; Zones, S. I. *Synthesis of Microporous Materials*; Occelli, M. L., Robson, H., Eds.; Van Nostrand Reinhold: NY, 1992; Vol. 1, p 222.
(45) Zones, S. I.; Darton, R. J.; Morris, R.; Hwang, S. J. *J. Phys. Chem. B* **2005**, *109*, 652–661.
(46) Gies, H. *Inclusion Compounds*; Academic Press: London, 1995; Vol. 5, p 1.
(47) Gies, H.; Marler, B. *Zeolites* **1992**, *12*, 42.
(48) Shvets, O. V.; Kasian, N.; Zukal, A.; Pinkas, J.; Čejka, J. *Chem. Mater.* **2010**, *22*, 3428–3495.
(49) Villaescusa., L. A.; Díaz., I.; Barrett., P. A.; Nair., S.; LLoris-Cormano., J. M.; Martínez-Mañez., R.; Tsapatsis., M.; Liu., Z.; Terasaki., O.; Camblor., M. A. *Chem. Mater.* **2007**, *19*, 1601–1612.
(50) (a) Treacy. M. M. J.; Deem. M. W.; Newsam. J. M. DIFFaX, version 1.801; 1995. (b) Treacy., M. M. J.; Newsam., J. M.; Deem., M. W. *Proc. R. Soc. London, Ser. A* **1991**, *433*, 499.